# METHODS OF REDUCTION OF WIND INDUCED DYNAMIC RESPONSE IN SOLAR CONCENTRATORS AND OTHER SMALL LIGHTWEIGHT STRUCTURES

Monte A. McGlaun
LaJet Energy Company

**ABSTRACT:**

Wind tunnel studies indicate that solar concentrator structures with low damping properties are susceptible to dynamic wind loading characteristic of the earth's boundary layer. Solar concentrators are sensitive to deflections in optical systems and can be costly when required to have minimal deflections. The cost and performance characteristics can be improved through structural design approaches to reduce dynamic response. This study evaluates the benefits of various methods to control dynamic response: passive damping, multiple supports, friction connections, mass alterations, and beam length modifications.

The Modal Strain Energy Method (MSEM) is an efficient analysis tool for evaluating overall structural damping on complex structures. Modal strain energies were found using a finite element analysis structural program. The MSEM was used to analyze the complex structure of the LaJet Energy LEC 1900 Solar Concentrator. MSEM methodologies are described in-depth.

Viscoelastic (passive) damping and bracing were found most efficient at reducing dynamic response in the structure. Braces were located to develop large modal strain energies. When bracing and damping were located to develop high modal strain energy for particular modes, system loss factors were notably improved. Damping was effective when radial girders were dynamically involved in the mode shape definition.

---

Monte A. McGlaun, P.E.
Director of R & D
LaJet Energy Company
3130 Antilley Road
Abilene, TX 79606
(915) 698-8800

## 1.0 INTRODUCTION

**1.1. PROJECT OBJECTIVE:** *To apply the modal strain energy method (MSEM) to design damping and bracing to achieve greater dynamic stabiltiy in a large solar concentrator dish.*

**1.2. FUNDING OF STUDY:** SBIR Program, DOE Contract No. DE-AC05-87/ER80519 DOE Report No. DOE/ER/80519-1

## 1.3. BACKGROUND

LaJet Energy has designed, built, tested, and marketed solar concentrators since 1978. In 1983 and with internal dollars and private funding LaJet Energy designed and buily SOLARPLANT 1, a solar thermal electric-generating power plant at Warner Springs, California with 700 LEC 460 solar concentrators.

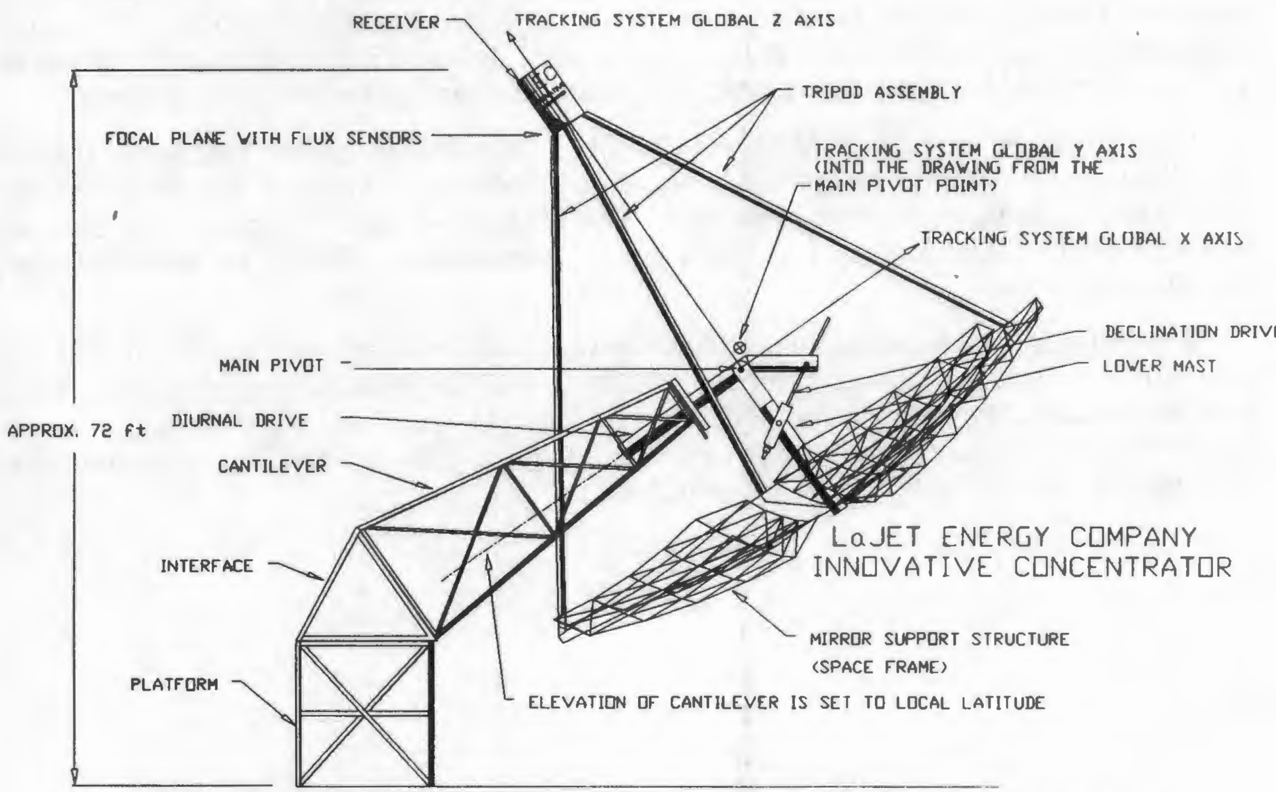


Figure 1 - LaJet Energy's DOE Innovative Concentrator Overall Side View (from the east)

LaJet Energy's solar concentrator technology is licensed to Cummins Power Generation (a wholly owned subsidiary of Cummins Engine Company) for worldwide sales for electrical production. Cummins is funding the commercialization of a free-piston Stirling engine - solar concentrator electrical production system. The project is in the second year of a five year program.

The structural design used in this study is designated the *Large Scale Innovative Concentrator* (IC). LaJet Energy designed the IC under U. S. Department of Energy (DOE) cost-share agreement (DE-FC04-85 ET30171).

The *IC* accommodates 95 silver polymer film mirrors to reflect $135kw_{th}$ through a 20 inch diameter aperture. Figure 1 shows the *IC* at solar noon and at the vernal or autumnal equinox. The structure is comprised of a stationary support system and a tracking support system. The platform, interface, and cantilever are the stationary structure. The lower mast, girders, space frames, mirror facets, tripods, and receiver are the tracking assembly.

The tracking functions are performed under microprocessor control that operates one or both of the two drive motors to keep the optical axis (global z axis) pointed to the sun. The array of concave mirrors reflects and focuses the incoming solar radiation into an opening in the bottom of the receiver. The receiver can be any device designed to accept concentrated solar radiation for a purpose such as creating steam, generating electricity, or high temperature materials processing.

## 2.0 STRUCTURAL LOADING

### 2.1. GRAVITY

The LaJet Energy solar concentrator structures have high strength-to-weight ratios; therefore, gravity loading is usually secondary to wind loading. Ice and snow loading in the northern tier locations may be large and require special design situations *(solar devices are more likely to be located in warmer climates).*

### 2.2. WIND

Wind is characterized as a spectral loading, and the majority of energy imparted occurs at excitation frequencies up to 30 Hz. Since solar dishes have very large surface areas, wind is the primary loading. Wind forces near the earth have a turbulent boundary layer with characteristics that depend on the roughness of the surrounding terrain. A model of the structure under study was tested in the boundary layer wind tunnel at Colorado State University to determine the loads at the main pivots of the tracking array but not the distributed loads [19].

### 2.3. APPLICATIONS

For example free piston Stirling engines are currently being tested on the LaJet Energy Concentrators by Cummins Power Generation. The engine operates at 60 Hz and a .5 mm amplitude. The mass of the associated engine mounting components on the solar concentrator reduce the amplitude by the inverse ratio of the masses. The concentrators have not exhibited destructive modes in the region of 60 Hz. Application dynamic loading is less of a design issue than gravity considerations.

### 2.4. SEISMIC

The primary destructive mode of seismic activity is through the application of lateral forces. Since the dish is designed for wind acting as a large lateral load and since the dish has a high strength-to-weight ratio, seismic loading is always evaluated by is typically a secondary factor of design.

## 3.0 ANALYTICAL MODEL DEVELOPMENT

### 3.1. FINITE ELEMENT ANALYSIS (IMAGES 3D)

IMAGES3D Finite Element Analysis Program is a copyright of Celestial Software, Inc., 125 University Avenue, Berkeley, CA 94710, telephone (415) 420-0300 [13]. The distribution of the components of the finite element model of the tracking portion of the *IC* is shown. All materials used in the *As-Designed* model were steel. The components of the *IC* have been sized, modeled, and constructed as shown in the tables following:

| | |
|---|---|
| 696 node points to describe the geometry | |
| 986 beam elements drawn from 20 different cross-sections | |
| 290 plate elements to describe the 18 inch diameter, 3/4 inch wall Lower Mast. | |
| Girders | 5.56" O.D. x .188" wall |
| Tripods | 8.625" O.D. x .188" wall |
| Space Frame Beams | a. 1.00" O.D. x .035" wall<br>b. 1.25" O.D. x .035" wall<br>c. 1.163" O.D. x .057" wall<br>d. 1.510" O.D. x .065" wall |
| Lower Mast | 18" O.D. x .75" wall |
| Simulated Engine Weight | 4,400 $lb_f$ at z = 509 inches |

Table 1 - Structural & FEM Components for the *As-Designed IC*

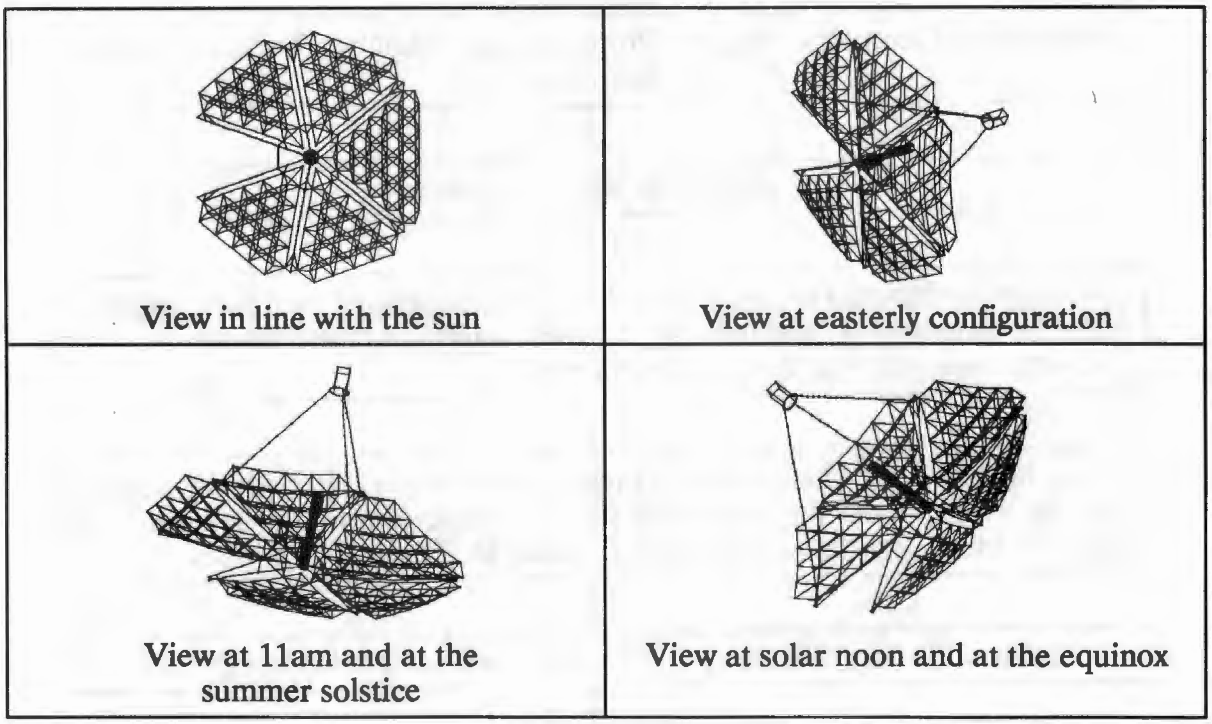


FIGURE 2 - IMAGES3D Plots of the *IC* Tracking System

FIGURE 3 - PHOTO OF *IC* IN THE ORIGINAL CONFIGURATION IN WESTERLY CONFIGURATIONS

## 3.2. MODAL STRAIN ENERGY COMPUTATION

Input Basic Geometry, Material Properties, and Member Properties of the Structure

Create the Stiffness Matrix

Calculate the Modal Frequencies and Shapes (number of modes is limited to 90 by the program). Computer disk storage capacity and the time necessary for computation will be the determining factor.

Leave IMAGES3D. Use an ASCII text editor to split the mode shapes into files each containing displacements for one mode shape and to permit the STATIC Module of IMAGES3D to calculate Modal Strain Energies.

Follow the program setup for the force induced Strain Energy Run

Reenter IMAGES3D for each Modal Strain Energy run desired and have the Element Modal Strain Energies written to files for post analysis.

Import the Element Modal Strain Energies into a high capacity spreadsheet. Apply material loss factors to each element and multiply times the element strain energy.

COMPUTE THE SYSTEM LOSS FACTOR

$$\eta_s^{(r)} = \frac{\sum_{k=1}^{n} \eta_k U_k^{(r)}}{\sum_{k=1}^{n} U_k^{(r)}} \qquad (1)$$

TABLE 2 - Modal Strain Energy Analysis Flow Chart

In the following tables, successive derived mode shapes are presented graphically. The center panel is the undeformed geometry, the left panel subtracts 100 times the modal deflections, and the right panel adds 100 times the modal deflection. Therefore, a sense of the computer mode shape animation can be derived from looking left to right. For the *As-Built* analysis the material loss factor, $\eta$, is taken at a very low value of .001 since all materials are metal.

## 3.3. AS-DESIGNED MODAL ANALYSIS

**MODE 1**

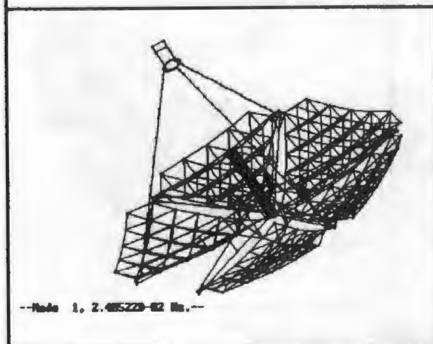

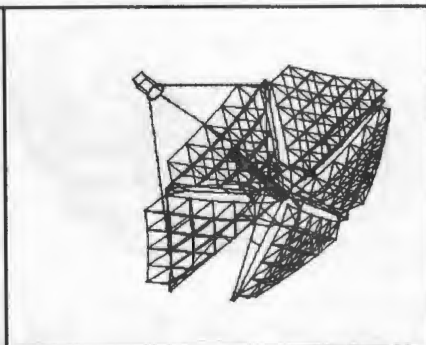

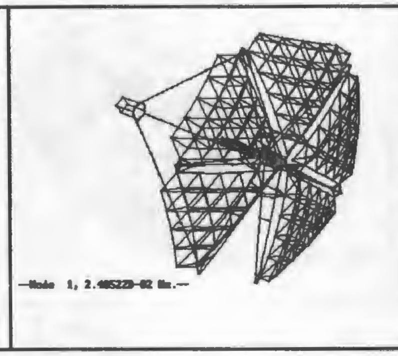

| | | | |
|---|---|---|---|
| System Loss Factor, $\sum \eta_k$ | 0.001 | Modal Frequency | 0.024052 Hz |
| System Strain Energy, $\sum U_k^{(r)}$ | 0.226287 | | |
| System Loss Product, $\sum \eta_k U_k^{(r)}$ | 0.000226 | | |

| Element | | | | Description | |
|---|---|---|---|---|---|
| No. | Strain Energy, $U_k^{(r)}$ | $\eta_k$ | Descending Sort of Component Loss Factors, $\eta_k U_k^{(r)}$ | Component | Portion of Component |
| 711 | 3.77028E-06 | 0.001 | 3.77028E-09 | GIRDER 1 | Top |
| 769 | 1.64302E-06 | 0.001 | 1.64302E-09 | GIRDER 3 | Top |
| 721 | 1.48344E-06 | 0.001 | 1.48344E-09 | GIRDER 1 | Mid Vert Tie |
| 719 | 1.45392E-06 | 0.001 | 1.45392E-09 | GIRDER 1 | Bottom |
| 712 | 1.28791E-06 | 0.001 | 1.28791E-09 | GIRDER 1 | Top |
| 710 | 1.26862E-06 | 0.001 | 1.26862E-09 | GIRDER 1 | Top |
| 722 | 1.26787E-06 | 0.001 | 1.26787E-09 | GIRDER 1 | Outboard Vert Tie |
| 718 | 1.23123E-06 | 0.001 | 1.23123E-09 | GIRDER 1 | Bottom |
| 776 | 9.42109E-07 | 0.001 | 9.42109E-10 | GIRDER 3 | Bottom |
| 708 | 9.02250E-07 | 0.001 | 9.02250E-10 | GIRDER 1 | Top |
| 768 | 8.78665E-07 | 0.001 | 8.78665E-10 | GIRDER 3 | Top |
| 766 | 7.76672E-07 | 0.001 | 7.76672E-10 | GIRDER 3 | Top |
| 715 | 7.38142E-07 | 0.001 | 7.38142E-10 | GIRDER 1 | Bottom |
| 779 | 6.75916E-07 | 0.001 | 6.75916E-10 | GIRDER 3 | Mid Vert Tie |
| 717 | 6.18575E-07 | 0.001 | 6.18575E-10 | GIRDER 1 | Bottom |
| 709 | 5.61057E-07 | 0.001 | 5.61057E-10 | GIRDER 1 | Top |
| 773 | 5.00326E-07 | 0.001 | 5.00326E-10 | GIRDER 3 | Bottom |
| 767 | 4.43813E-07 | 0.001 | 4.43813E-10 | GIRDER 3 | Top |
| 775 | 3.82166E-07 | 0.001 | 3.82166E-10 | GIRDER 3 | Bottom |
| 777 | 3.66264E-07 | 0.001 | 3.66264E-10 | GIRDER 3 | Bottom |

Figure 4 - Undamped Mode Shape 1 of *As-Designed IC*

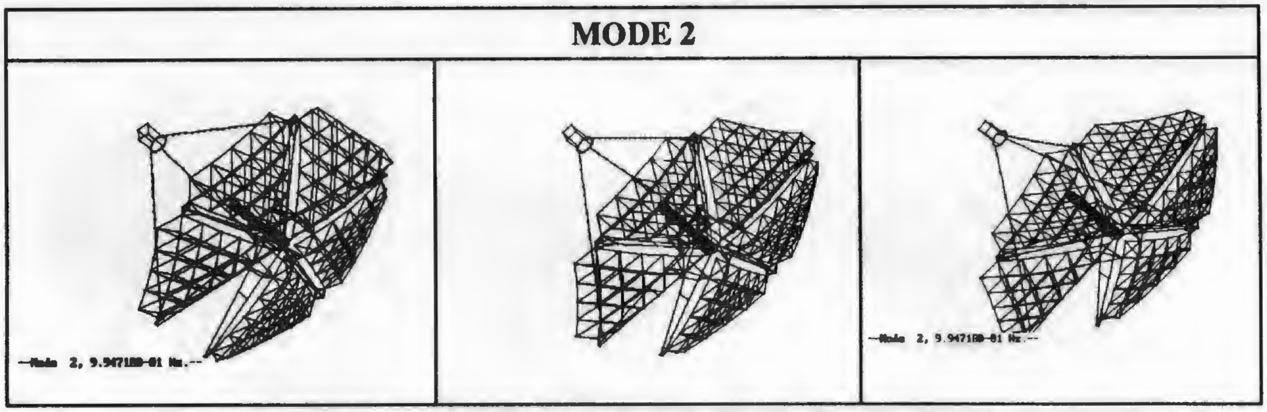


Figure 5 - Undamped Mode Shape 2 of *As-Designed IC*

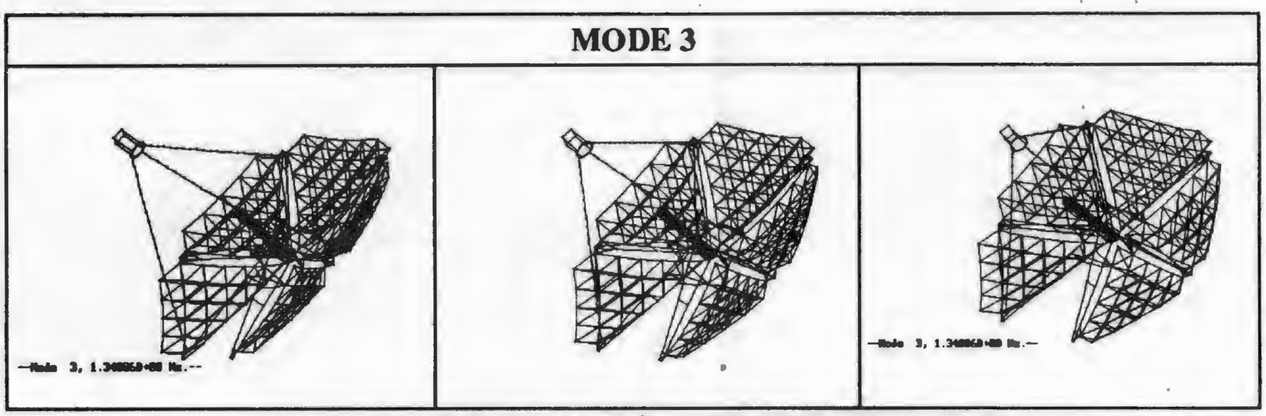


Figure 6 - Undamped Mode Shape 3 of *As-Designed IC*

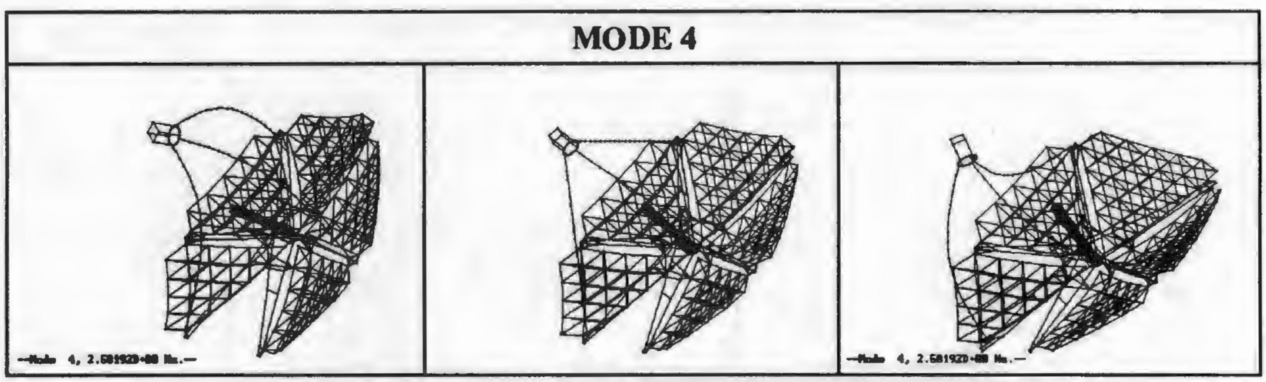


Figure 7 - Undamped Mode Shape 4 of *As-Designed IC*

**MODE 5**

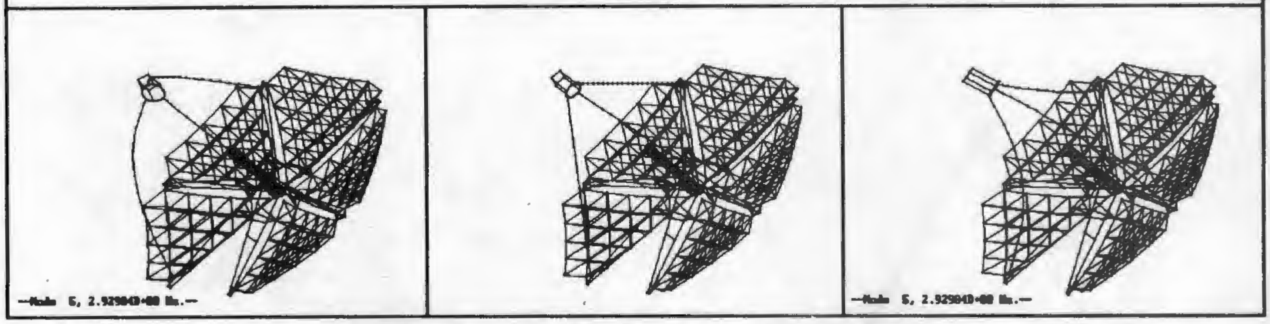

Figure 8 - Undamped Mode Shape 5 of *As-Designed IC*

## 4.0 STRUCTURAL BRACING AND DAMPING

Figures show stiffeners and dampers for the Girders and Tripods on the Innovative Concentrator. Two options were analyzed: *stiffeners only* and *stiffeners with dampers*. A choice was made based on experience with the *IC* structure to install stiffeners and dampers sized as shown in the Table.

| | |
|---|---|
| Stiffeners | 3" O.D. with .086" wall, A=.7854 $in^2$, I=.8345 $in^4$ |
| Viscoelastic Dampers | 6" O.D. with A=28.3 $in^2$, I=3.98 $in^4$, thickness=.25" of $\eta$ = 1.0 material, Two .375" steel plates |

Table 3 - Stiffener and Damper Selections

| | |
|---|---|
| Young's Modulus, linear elastic | $E$ = 1.083 ksi |
| Weight density | $\rho_w$ = .001 $lb_f/in^3$ |
| Poisson's Ratio | $\nu$ = .3 |
| Shear Modulus, linear elastic | $G_s$ = .417 ksi |
| Coeff. of Thermal Expansion | Not Used |

Table 4 - Viscoelastic Material Properties Used in FEA

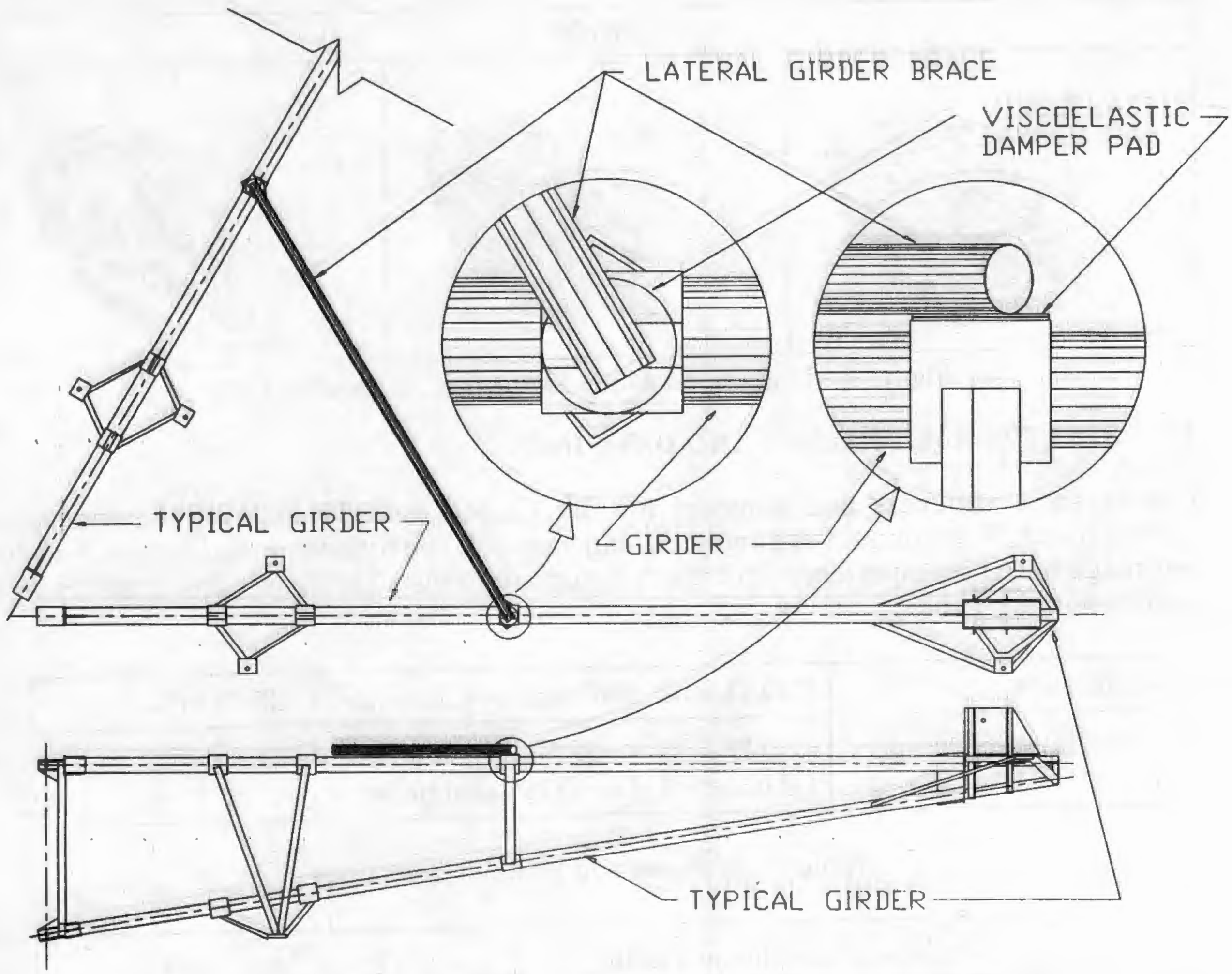


**Figure 9 - Stiffening & Damping of Lateral Modes in the Girders**

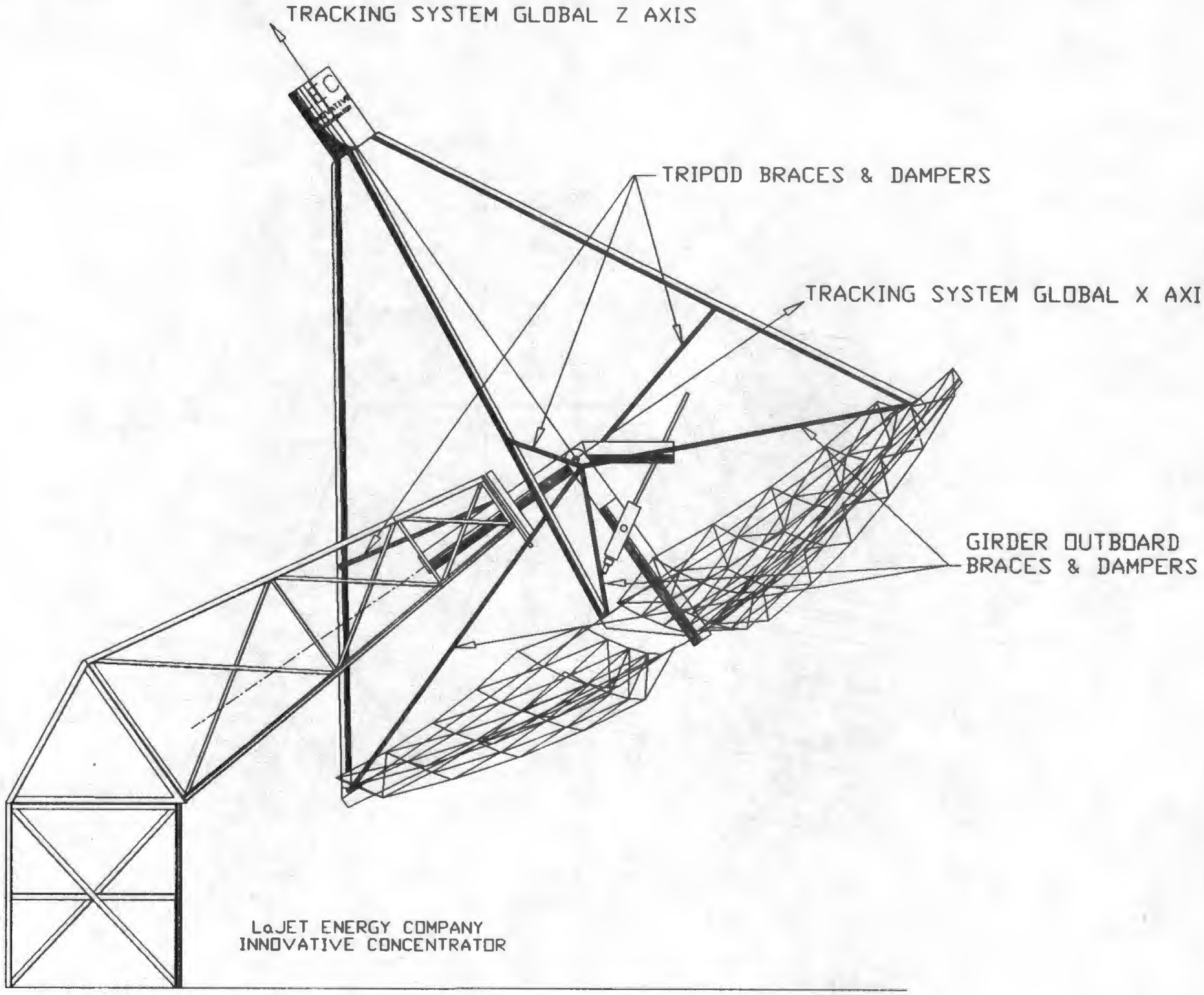


**Figure 10 - Tripod In-Plane & Girder Vertical Stiffeners & Dampers**

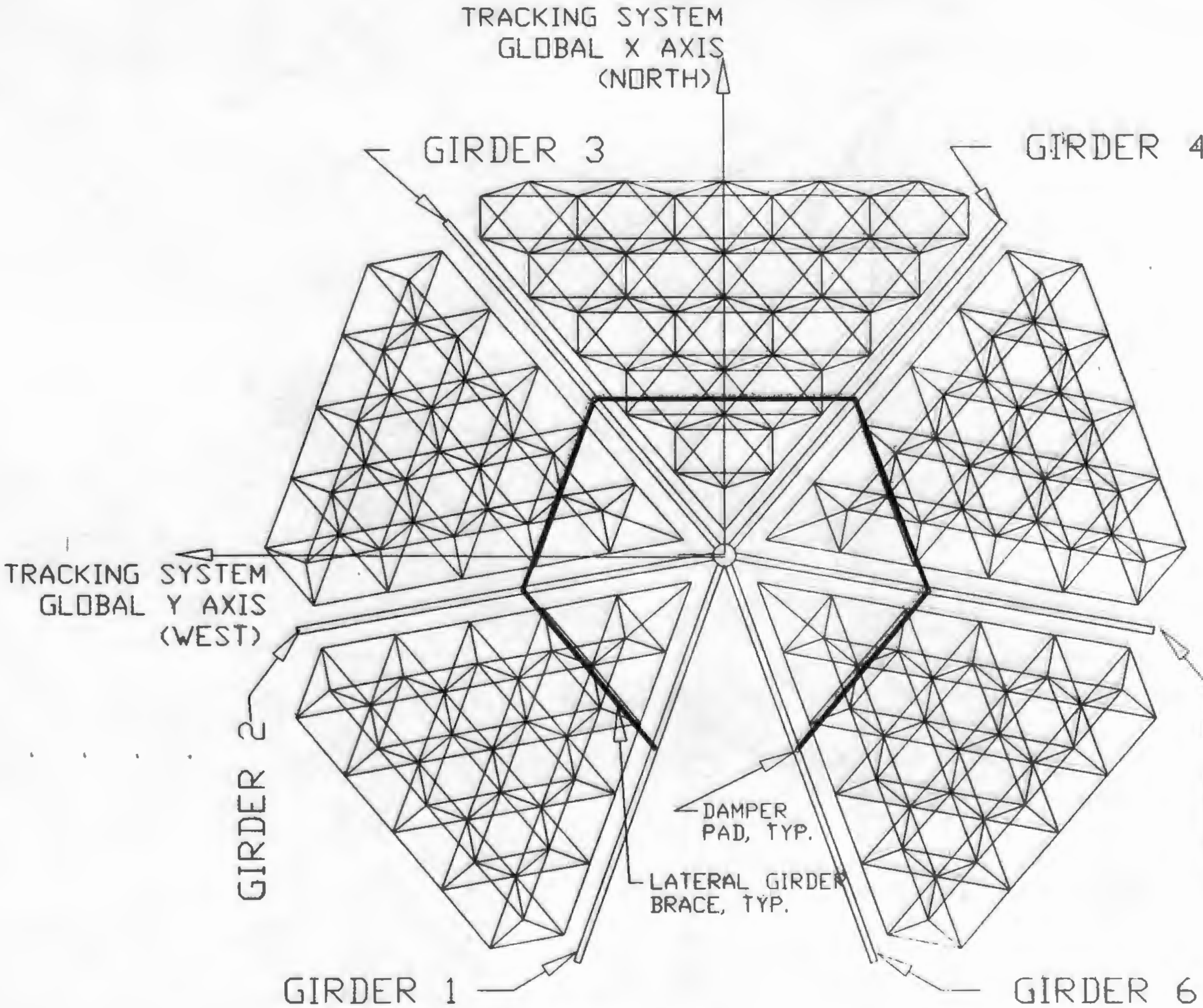


Figure 11 - Girder Lateral Stiffener Positions

## 5.0 DAMPED AND STIFFENED RESULTS

The following mode is a typical indication that the damper location was selected correctly to develop largest strain energies. With the high loss factors of a viscoelastic damper, the loss product sum for the structure is much larger than for the undamped structure. Note that the system loss factor is dramatically increased with the addition of a dampers in relatively few locations.

**MODE 5**

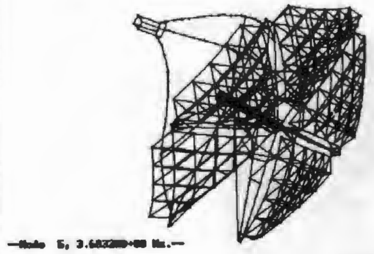

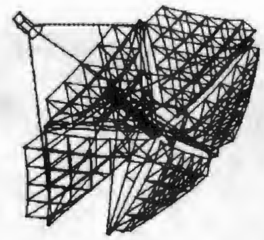

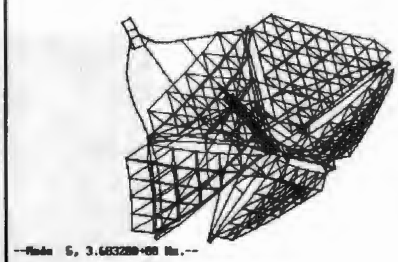

| | | | |
|---|---|---|---|
| System Loss Factor, $\sum \eta_k$ | 0.16739 | Modal Frequency | 3.68319 Hz |
| System Strain Energy $\sum U_k^{(r)}$ | 1.774E+03 | | |
| System Loss Product, $\sum \eta_k U_k^{(r)}$ | 2.970E+02 | | |

| Element | | | | Description | |
|---|---|---|---|---|---|
| No. | Strain Energy, $U_k^{(r)}$ | $\eta_k$ | Descending Sort of Component Loss Factors, $\eta_k U_k^{(r)}$ | Component | Portion of Component |
| 982 | 2.20234E+02 | 1 | 2.20234E+02 | DAMPER | Girder 3 Outbrd Active |
| 988 | 1.56167E+02 | 0.001 | 1.56167E-01 | BRACES | Girder 3 Outbrd |
| 766 | 5.80972E+01 | 0.001 | 5.80972E-02 | GIRDER 3 | Top |
| 980 | 5.07246E+01 | 1 | 5.07246E+01 | DAMPER | Girder 1 Outbrd Active |
| 773 | 3.83241E+01 | 0.001 | 3.83241E-02 | GIRDER 3 | Bottom |
| 986 | 3.65928E+01 | 0.001 | 3.65928E-02 | BRACES | Girder 1 Outbrd |
| 776 | 3.48538E+01 | 0.001 | 3.48538E-02 | GIRDER 3 | Mid Vert Tie |
| 907 | 2.92025E+01 | 0.001 | 2.92025E-02 | POD 1 | |
| 906 | 2.39679E+01 | 0.001 | 2.39679E-02 | POD 1 | |
| 765 | 2.21329E+01 | 0.001 | 2.21329E-02 | GIRDER 3 | Top |

Figure 12 - MODE SHAPE 5 OF DAMPED AND STIFFENED *IC*

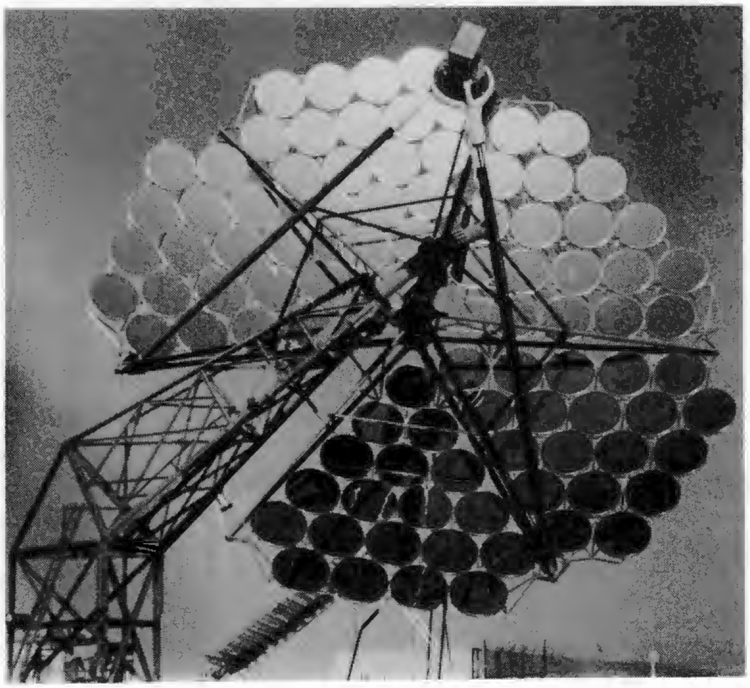

FIGURE 13 - PHOTO OF *IC* IN THE STIFFENED CONFIGURATION

The modal frequency of a single degree-of-freedom mass-spring-damper system is $\omega = (k/m)^{1/2}$. Therefore, it is to be expected that the addition of bracing to the Innovative Concentrator structure will raise the modal frequencies. Since hysteretic damping is modeled as a very low stiffness element within the finite element model, damping should reduce the modal frequencies below the *stiffened only* model. The Figure below is a plot of the modal frequencies for the three cases analyzed and for the first fifteen modes, and shows that the expected trends in modal frequency occur as expected. The frequencies follow the same general tendency until Mode 10 where the Tripod excitation dominates the response. In the *stiffened only* and *damped and stiffened* runs, the Tripod members are braced which raises the resonant frequency.

Modes 1 and 2 are essentially the same for all the structural cases explored. Mode 1 has a 41.7 second period which is accompanied by low excitation energy. Mode 2 is readily observed on both the LEC 460 and the IC and is a gross rotation about the z-axis (optical axis) of the dish. The z-rotation results in a widely distributed low stress level.

Dampers on the *in-plane* Tripod braces did not develop large strain energies for any of the modes. Consequently, where the mode shapes involved large modal activity of the Girders, the system loss factor was high. Conversely, if the Tripod modal strain energies dominated the mode shape summary, then the system loss factor was low. The graph in Figure below shows the system loss factor for each Mode. Note that Modes 3, 5, 6, 7, 9, and 10 have large Girder related modal strain energies and, as a result, have larger system loss factors.

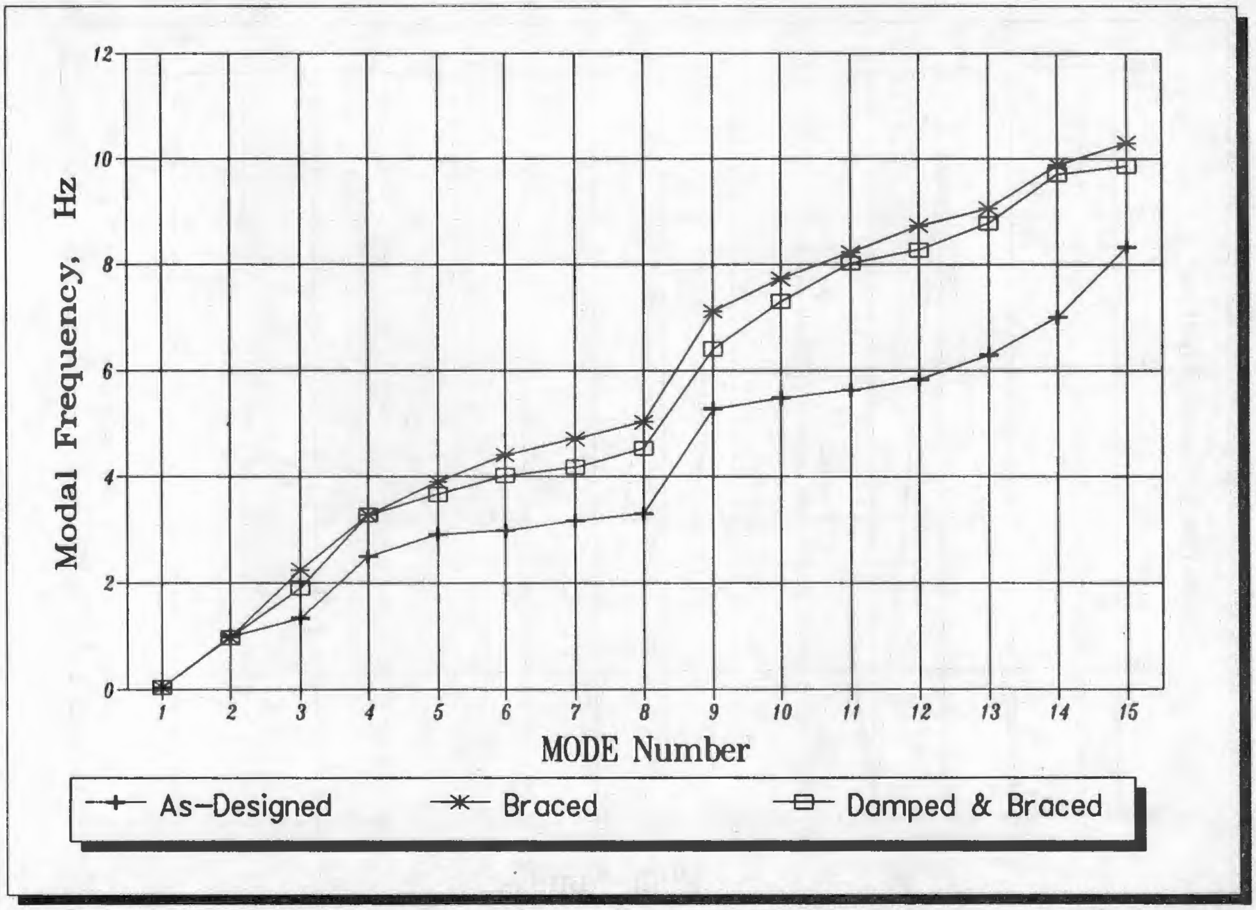


**Figure 14 - Modal Frequencies**

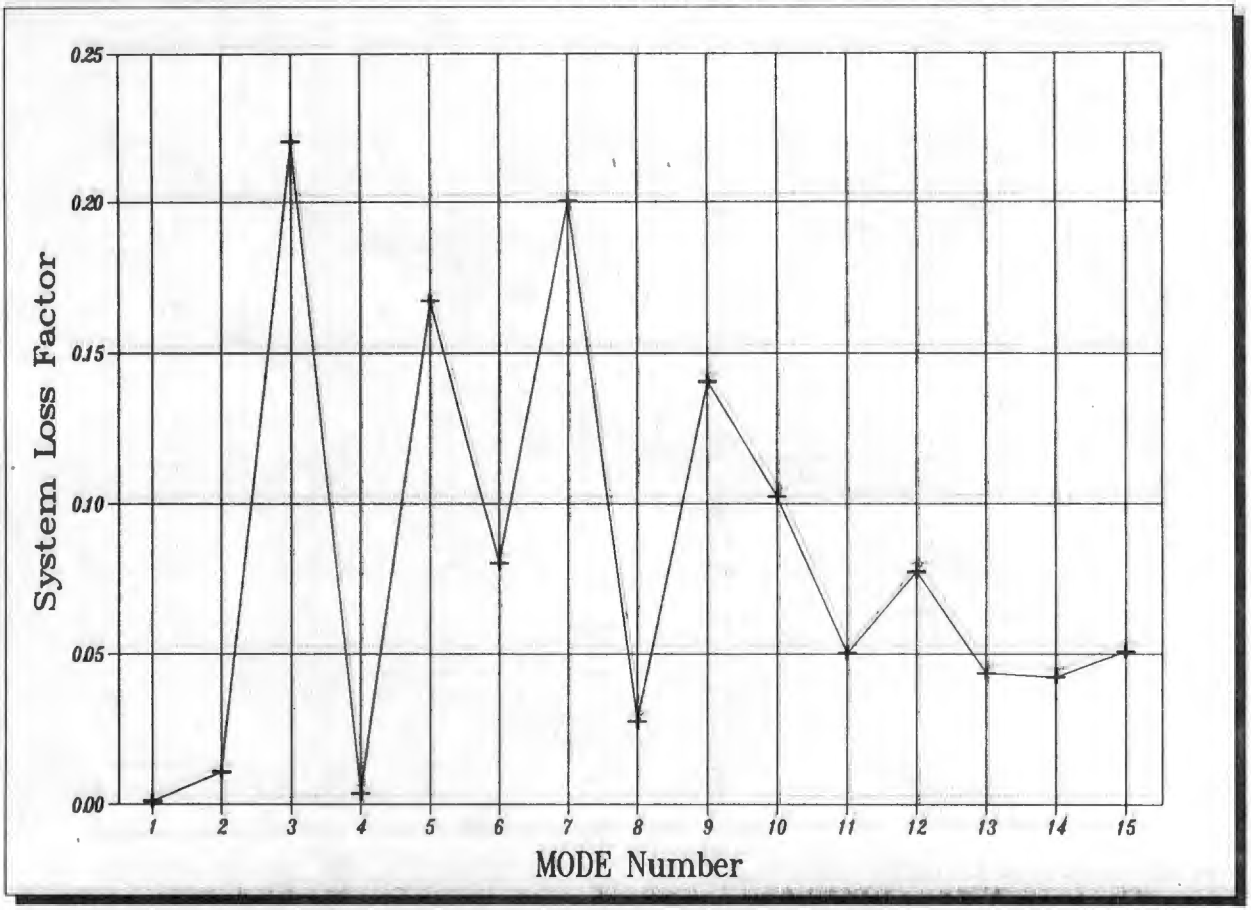


Figure 15 - System Loss Factors vs. Mode Numbers

Modal strain energy is developed in all portions of the structure. The Lower Mast was modeled with plate elements while the balance of the structure was modeled with beam elements. The strain energy associated with the Lower Mast was lower for all modes but Modes 1 and 2. Damping would be difficult to apply to the Lower Mast, and its lower modal strain energy values indicate that damping the Lower Mast would be marginally effective in increasing the system loss factor and reducing dynamic response. Therefore, damping was not considered for the Lower Mast in this study. The Figures below show the total modal strain energy by mode for both beam and plate elements for each analysis.

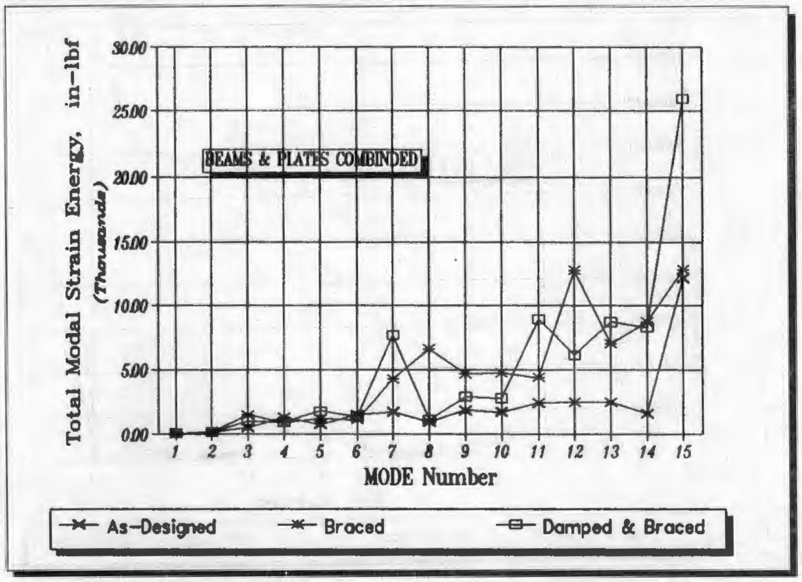


Figure 16 - Total Modal Strain Energy by Mode Number

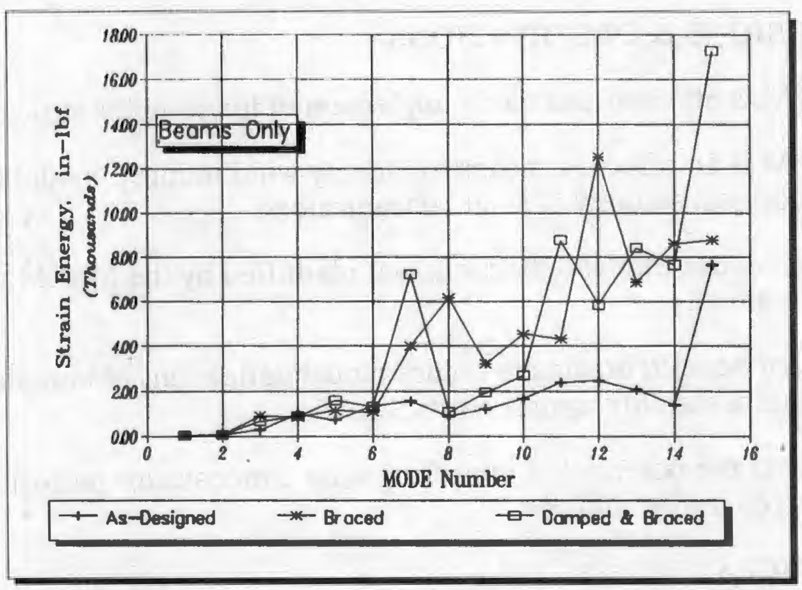


Figure 17 - Total Beam Modal Strain Energy by Mode Number

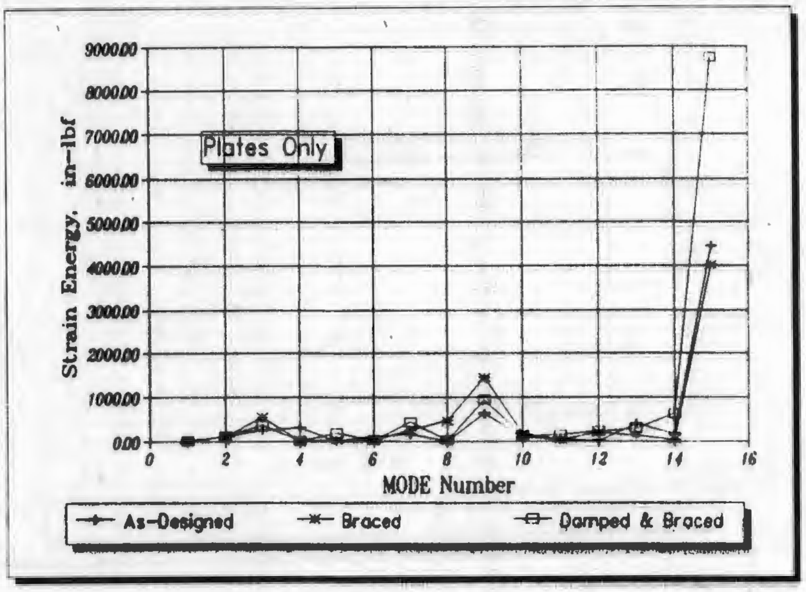


Figure 18 - Total Plate Modal Strain Energy by Mode Number

## 6.0 CONCLUSIONS & OBSERVATIONS

- The MSEM is efficient and easily implemented for complex structures.
- The MSEM is an effective means to identify wind induced modal deflections that can effect the optical stability of solar concentrators.
- Bracing to reduce modal deflections was identified by the MSEM was installed on the structure studied.
- As an added benefit, bracing to reduce modal deflections of long slender elements will provide lateral stability against elastic buckling.
- Damping has the potential of improving solar concentrator performance, survivability, durability, reliability, and cost.

## 7.0 REFERENCES


1. Cermak Peterka Peterson, Inc., *Analysis and Review of Field Test Data from the LaJet LEC-460 Collector*, April 1987, prepared for Sandia National Labs, Albuquerque, NM.
2. Chen, W.F., and Lui, E.M., Structural Stability, Elsevier Science Publishing Co., Inc., NY, 1987.
3. Clough, R.W. and Penzien, J., Dynamics of Structures, McGraw-Hill, Inc., NY, 1975.
4. Davenport, A.G., Isyumov, N., Rothman, H., and Tanaka, H., *Wind-Induced Response of Suspension Bridges - Wind Tunnel Model and Full Scale Observations*, Wind Engineering, Proceedings of the Fifth International Conference, Cermak, J.E. (ed.), Fort Collings, CO, July 1979, Pergamon Press, Oxford, 1980, Vol. 2, pp. 807-824.
5. Drake, M.L. and Bouchard, M.P., "On Damping Of Large Honeycomb Structure," *Journal Of Vibration, Stress, and Reliability in Design*, Vol.107, 361-366.

6. Drake, M.L., and Kluesener, M.F., "Finite Element Methods For Passive Damping Design," presented at ASME Intl. Computers in Engineering Conference, Boston, MA, Aug. 1985, Vol. 2 (Bk. No. GO286B).
7. Dynamic Stability of Large Structures: Non-Structural Viscoelastic Dampers, Product Design and Selection Guide, 3M Company, Structural Products Department, Industrial Specialties Division/3M, 230-1F-02 3M Center, St. Paul, MN 55144-1000.
8. IMAGES3D, Finite Element Analysis Program Manual, Celestial Software, Inc., 125 University Avenue, Berkeley, CA 94710.
9. Johnson, C.D., and Kienholz, D.A. and Rogers, L.C., "Finite Element Prediction Of Damping In Beams With Constrained Viscoelastic Layers," *The Shock and Vibration Bulletin*. 51, Pt. 1, 71-81 (May 1981).
10. Johnson, C.D., and Kienholz, D.A., "Finite Element Prediction Of Damping In Structures With Constrained Viscoelastic Layers," *AIAA Journal*, 20(9), 1284-1290, (September 1982).
11. Kluesener, M.F., "Results Of Finite Element Analysis Of Damped Structures," presented at Vibration Damping Workshop, Long Beach, CA, Feb. 1984.
12. Kluesener, M.F., and Drake, M.L., "Damped Structure Design Using Finite Element Analysis," *The Shock and Vibration Bulletin*., 52, Pt. 5, 1-12 (May 1982).
13. Leung, W.H., IMAGES3D, Finite Element Analysis Program Technical Reference Manual, Version 1.4, Celestial Software, Inc., 125 University Avenue, Berkeley, CA 94710.
14. Mahmoodi, P., and Keel, C.J,, "Performance Of Viscoelastic Structural Dampers for the Columbia Center Building", 3M Company, technical reference catalog titled *Effective Damping of Large Structures*.
15. Nashif, A.D., Jones, D.I.G., and Henderson, J.P., Vibration Damping, Wiley-Interscience, John Wiley & Sons, Inc., NY, 1985.
16. Soni, M.L., Kluesener, M.F. and Drake, M.L., "Damping and Control of Spacecraft Structures Using Synthesis and Damped Design for Flexible Spacecraft Structures," *Computers & Structures*, Pergamon Press Ltd., 1985, Vol. 20, No. 1-3, pp. 563-574.
17. Soni, M.L., "Finite Element Analysis of Viscoelastically Damped Sandwich Structures," *The Shock and Vibration Bulletin*., 51, Pt. 1, 97-108 (May 1981).
18. Strachan, J. W., *LaJet Wind Load Tests*, informal report, Solar Thermal Test Facility, Sandia National Laboratories, Albuquerque, NM (no date).
19. Thoroddsen, S.T., Peterka, J.A., and Cermak, J.E., "Wind Tunnel Study of Wind Loads on LaJet Solar Collector Model". CSU Project 2-96350, November 1985, Fluid Dynamics and Diffusion Laboratory, Colorado State University, Fort Collins, CO 80523.
20. Ungar, E.E., and Kerwin, E.M., Jr., "Loss Factors of Viscoelastic Systems in Terms of Energy Concepts," *Journal of the Acoustic Society of America*, Vol. 34, July 1962, pp. 954-957.
21. Zienkiewicz, O.C., The Finite Element Method, 3/e, McGraw-Hill Book Company (UK) Limited, Maidenhead Berkshire, England, 1977.